mathematics

MDPI

Article

Local and Global Dynamics of a Constraint Profit Maximization for Bischi–Naimzada Competition Duopoly Game

Sameh S Askar [1,2,*] and Abdulrahman Al-Khedhairi [1]

[1] Department of Statistics and Operations Research, College of Science, King Saud University, Riyadh 11451, Saudi Arabia; akhediri@ksu.edu.sa

[2] Department of Mathematics, Faculty of Science, Mansoura University, Mansoura 35516, Egypt

* Correspondence: saskar@ksu.edu.sa or s.e.a.askar@hotmail.co.uk

Received: 21 July 2020; Accepted: 28 August 2020; Published: 31 August 2020

Abstract: The Bischi–Naimzada game is a market competition between two firms with the objective of maximizing profits under limited information. In this article, we study a more generalized and realistic situation that takes into account the sales constraints. we generalize the economic model suggested by Bischi–Naimzada by introducing and studying the maximization of profits based on sales constraints. Our motivation in this paper is the studying of profit and sales constraints maximization and their influences on the game's dynamics. The local stability of the equilibrium points of the proposed model is discussed. It examines how the dynamics of the proposed two-dimensional competition game model focusing on changes in both the speed of the adjustment and the sales constraint parameters. The map describing the game is proven to be noninvertible and yields many multi-stable, complex dynamics and the coexistence chaotic attractors may arise. The global behavior of the map is achieved by studying the critical curves. The numerical simulations demonstrate the coexistence of two attractors and complex structures of the attraction basins. Several examples are discussed in order to confirm all the analytical results obtained.

Keywords: Bischi–Naimzada game; bounded rationality; flip bifurcation; critical curves; basin of attraction; noninvertible map

1. Introduction

Oligopoly is a competition game where the market situation is controlled by a few competing firms producing similar or homogeneous products. The concept of static competition of duopoly game was first presented by Cournot [1]. The duopoly model is a competitive game where two companies control and have a dominant influence on the market. A typical feature that many articles share is the assumption of oligopoly model activities in order to maximize profit function as a single goal [2]. The game strategy of each company is related to each other and depends not only on market demand, but also on the planning expectations of the competitor. The pioneering contribution of Puu's work [3] has shown the potential for the complex dynamics of the duopoly competition of Cournot game. In literature [4–10], the dynamic behaviors and chaos of Cournot models have been discussed on the basis of naive expectations. Subsequently, an analysis of the global dynamics of the Cournot Competition game with bounded rationality was presented by Bischi and Naimzada [11]. All of these models have shown that equilibrium points could lose their stability, leading to periodic or chaotic behavior. Recently, the stability and complexity of Cournot competition games with limited rationality attracted more attention of researchers.

In this paper, we analyze the Bischi–Naimzada duopoly game based on firms considering a profit maximizer under a sales constraint. Taking into account that the sales constraint is a more

realistic economic situation than maximizing the only firm's profit. Such an added objective motivates our contribution in the current paper and can improve and extend the region of stability for the Nash equilibrium point. Furthermore it generalizes other existing models in literature. We study the stability of the dynamic equilibrium point leading to an in-depth understanding of the dynamics of the game and the corresponding economic interpretations. We use stability criteria as well as the numerical simulation to determine the local and global stability of the equilibrium points as well as to discuss the internal complexity of the game. Indeed studying the model according to the parameters of the speed of adjustment mechanism and the parameters of the sales constraints that we propose is capable of leading the model to different cycles or forms of complex dynamics involving potential economic instability. On the other hand, small perturbations of related standards may lead to sudden jumps from one attraction basin to another, based on the complexity of the basin structures and the phenomena of coexistence even in the absence of chaos. We obtain the critical curves of the non-invertible map, and it turns out that a sequential change in game's parameters leads to the collapse of game. Moreover, the behaviors of destabilization also involve a subcritical period doubling bifurcation, some periodic, aperiodic and chaos has been merged with an increase in the speed of adjustment parameters. In particular, we show that if the sales constraint parameters are taken to be high, this makes Nash equilibrium point goes back to local stability and has a reflective effect of increasing the model's adjustment speeds.

This paper is divided as follows. In Section 2, we report related works in this direction of research. In Section 3, the Bischi–Naimzada duopoly game based on maximizing profits and sales constraints is introduced. In Section 4, the local stability conditions for the equilibrium points are determined. In Section 5, numerical simulation, local bifurcations, basin of attraction, critical curves and path to complex dynamics are investigated. Finally, the conclusion and discussion are set out in Section 6.

2. Literature Review

Research on the complex dynamics of competition games may be classified according to the type of model or the number of players or the type of players expected to be homogeneous and heterogeneous. Agiza et al. [12,13] analyzed the dynamics of two oligopolistic games based on a limited rationality with a linear and nonlinear demand function. Bischi et al. [14,15] investigated chaos and bifurcations in two dynamic oligopoly games. The oligopoly was presented in the economic models of heterogeneous expectations explored in [13,14]. A multi-market game based on Puu's approach [16] has been introduced in [17]. Fanti et al. [18] examined the local and global dynamics of a homogeneous Cournot duopoly game with isoelastic demand function. Askar and Al-Khedhairi [19] analyzed the nonlinear duopoly games with product differentiation. Ma et al. [20] analyzed the complex behaviors and applied useful control of chaos to master-slave duopoly game. Agliari et al. [21] studied the dynamics of a differentiated Cournot duopoly game. Askar [22] explored the dynamics of Cournot duopoly game based on uncertainty cost. Andaluz et al. [23] studied the dynamic of triopoly Cournot and Bertrand games with differentiated products and heterogeneous expectations. Baiardi and Naimzada [24] investigated the dynamics of evolutionary Cournot oligopoly game with imitators. The dynamic behaviors of the two-stage Cournot duopoly model with an RD spillover effect have been studied in [25]. Al-Khedhairi [26] introduced the Cournot duopoly game with a generalized bounded rationality. The influences of asymmetric market information on the dynamics of duopoly game have been explored in [27]. Other interesting papers have been published in the literature, such as the works by Naimzada and Sbragia [28] which has studied oligopoly games with nonlinear demand and cost functions. Tramontana [29] has examined heterogeneous duopoly based on isoelastic demand. Askar [30] has analyzed Cournot–Bertrand game with differentiated goods. The dynamic of oligopoly games with goods differentiation discussed in [31]. The dynamics of differentiated Bertrand duopoly game investigated in [32]. The complex dynamics of delayed Bertrand duopoly game explored in [33]. A remanufacturing duopoly model with nonlinear cost studied in [34]. Effect of information asymmetry in the bounded Cournot duopoly game discussed by Ueda [35].

All competed firms in the works mentioned above were trying to maximize their profit functions without constraints as unique objectives. Baumol [36] presented an alternative model of increased sales as the company increases its sales on the basis of a minimum profit. Fischer [37,38] concluded that the idea of maximizing profits subject to minimum sales constraints was much more rational for business. More recently, Ahmed et al. [39–41] introduced dynamic multi-objective games as an alternative to firms which think with a single objective optimization. Mert [42] studied the duopoly model with two objectives to increase sales and maximize profits, giving Nash equilibrium a more stable when it comes to maximizing sales and profits rather than maximizing profit. Ibrahim [43] achieved the stability conditions for the Nash equilibrium point in the duopoly model with minimum sales constraints. Tian et al. [44] investigated coordination and control of multi-channel supply chain based on consumers' channel preferences and sales effort. Pansera et al. [45] studied bifurcation analysis of a delayed duopoly game with R&D spillover and price competition. More recently, the book includes new directions for nonlinear dynamics in games, see [46]. In [47], the price and quantity that are traded off between buyer and seller have been determined in bilateral monopoly. Investigation of excessive competition and a lack of trust and their influences that may affect rational choice in coalitional game have been analyzed in [48].

3. Bischi–Naimzada Duopoly Game under Minimum Sales Constraint

Assuming a market dominated by two firms producing homogeneous or same products. Let q_i be the output of firm $i = 1, 2$ and $Q = q_1 + q_2$ denotes the total output of the two firms. Suppose that the market demand function is linear in form [11]:

$$p = a - b(q_1 + q_2) \tag{1}$$

where p indicates the price of the products. We assume that both firms adopt the following linear cost function,

$$C_i(q_i) = c_i q_i \tag{2}$$

Since the total profit for the firm is the total revenue minus the total cost, the profit for each firm is given by

$$\pi_i\left(q_1, q_2\right) = q_i(a - bQ) - c_i q_i \tag{3}$$

Assuming that firms have a constant constraint on minimum sales constraint [43]. The firm i believes that it maximizes its profit under the condition on sales constraint, then we have the following optimization problem

$$\text{maximizes} \quad q_i(a - bQ) - c_i q_i \quad \text{subject to} \quad q_i(a - bQ) \geq S_i, \tag{4}$$

It is equivalent to maximize the payoff function as the objective function of firm i, which has the form

$$L_i = q_i(a - bQ) - c_i q_i - \mu_i \left(q_i(a - bQ) - S_i\right), \tag{5}$$

where the parameter μ_i is positive and is associated with the sales constraint. By differentiating L_i with respect to q_i, we obtain

$$\frac{\partial L_i}{\partial q_i} = (1 - \mu_i)(a - 2bq_i - bq_{-i}) - c_i = 0, i = 1, 2. \tag{6}$$

The objective of each firm is to maximize its profit on the basis of minimum sales constraints. The objective is therefore to maximize the function defined in (5) which combines the function of profit with the constraints of sales.

The Dynamic Game

We consider the situation where each firm adopts the same mechanism in adjusting its output in next period of time. We are of the opinion that these two firms are rationally limited, that is, they have limited information, each from the other, so that they will decide their outputs depending on the local estimation behavior of the objective function during the period [11–13]. Thus, the dynamic system that describes this game is in the form:

$$q_i(t+1) = q_i(t) + \nu_i q_i(t) \frac{\partial L_i}{\partial q_i}, i = 1, 2. \tag{7}$$

where $\nu_i > 0$ represents the adjustment speed of firm i.

Substituting (6) in (7), the dynamics of the two firms' outputs through a discreet dynamical system will be as follows:

$$\begin{array}{l} q_1(t+1) = q_1(t) + \nu_1 q_1[(1-\mu_1)(a - 2bq_1 - bq_2) - c_1] \\ q_2(t+1) = q_2(t) + \nu_2 q_2[(1-\mu_2)(a - 2bq_2 - bq_1) - c_2] \end{array} \tag{8}$$

The game mentioned above and described by the map (8) is a generalization of the Bischi–Naimzada game [11] when there is a constraint on sales. The system described in (8) determines the trajectories of competing firms, and it is a noninvertible two-dimensional map as shown later. We are investigating the dynamics of the model by discussing the effect of the parameters on this system. In order to address the dynamical behavior (8), we analyze the stability regions and the bifurcation of the equilibrium points by which the points may be destabilized.

4. Equilibrium Points and Their Local Stability

To obtain the fixed points for the model (8), the fixed point conditions $q_1(t+1) = q_1(t) = q_1^*$ and $q_2(t+1) = q_2(t) = q_2^*$, are used,

$$\begin{array}{l} q_1[(1-\mu_1)(a - 2bq_1 - bq_2) - c_1] = 0, \\ q_2[(1-\mu_2)(a - 2bq_2 - bq_1) - c_2] = 0 \end{array} \tag{9}$$

Solving the algebraic system (9), we get the following four fixed points of the system (8):

$$\begin{array}{l} E_0 = (0,0), \ \ E_1 = (\frac{a(1-\mu_1)-c_1}{2b(1-\mu_1)}, 0), \ \ E_2 = (0, \frac{a(1-\mu_2)-c_2}{2b(1-\mu_2)}), \\ E_* = (q_1^*, q_2^*) = \left(\frac{a(1-\mu_1)(1-\mu_2)+c_2(1-\mu_1)-2c_1(1-\mu_2)}{3b(1-\mu_1)(1-\mu_2)}, \frac{a(1-\mu_1)(1-\mu_2)+c_1(1-\mu_2)-2c_2(1-\mu_1)}{3b(1-\mu_1)(1-\mu_2)} \right) \end{array} \tag{10}$$

E_0, E_1, E_2 are called boundary equilibria and E_* is the Nash equilibrium. They have all non-negative real values which hold under the following inequalities:

$$\begin{array}{l} 2c_1(1-\mu_2) - c_2(1-\mu_1) < a(1-\mu_1)(1-\mu_2), \\ 2c_2(1-\mu_1) - c_1(1-\mu_2) < a(1-\mu_1)(1-\mu_2). \end{array} \tag{11}$$

It should be noted that the Nash equilibrium point E_* of the game (8) is the same of the Bischi–Naimzada game [30] when $\mu_1 = \mu_2 = 0$.

To study the local stability of those points we should calculate the Jacobian matrix of system (8) that is given by,

$$J = \begin{bmatrix} 1 + \nu_1[(1-\mu_1)(a - 4bq_1 - bq_2) - c_1] & -\nu_1(1-\mu_1)bq_1 \\ -\nu_2(1-\mu_2)bq_2 & 1 + \nu_2[(1-\mu_2)(a - 4bq_2 - bq_1) - c_2] \end{bmatrix}, \tag{12}$$

whose characteristic polynomial is as follows,

$$f(\lambda) = \lambda^2 - tr(J(E))\lambda + det(J(E)), \tag{13}$$

where tr(J) and det(J) are the trace and determinant of the matrix (12), respectively. The conditions for achieving the local asymptotic stability of the Nash equilibrium point are that the eigenvalues of the corresponding Jacobian matrix are within the unit circle. According to the Jury criterion [49,50], the conditions of local asymptotic stability of the Nash equilibrium point can be described in detail as

$$\begin{array}{l} f(-1) = 1 + tr(J(E)) + det(J(E)) > 0, \\ f(1) = 1 - tr(J(E)) + det(J(E)) > 0, \\ det(J) < 1. \end{array} \tag{14}$$

Breaking any of the inequities mentioned in (14) while realizing the other two at the same time, leads to:

- Flip bifurcation at $f(-1) = 0$,
- Transcritical or fold bifurcation at $f(1) = 0$,
- Neimark–Sacker bifurcation at $\det(J) = 1$.

It is clear that the system (8) is a nonlinear system and therefore it is difficult to obtain an explicit time-dependent solution. From this point of view, we will study the specific behaviors of this model by applying the stability theory around the equilibrium points.

Theorem 1. *The equilibrium point E_0 of the two firms outside the market is*

- *a repelling node if* $a > \max\{\frac{c_1 - 1}{\nu_1(1-\mu_1)}, \frac{c_2 - 1}{\nu_2(1-\mu_2)}\}$,
- *an attracting node if* $a < \min\{\frac{c_1 - 1}{\nu_1(1-\mu_1)}, \frac{c_2 - 1}{\nu_2(1-\mu_2)}\}$,
- *a saddle node if* $a > \frac{c_1 - 1}{\nu_1(1-\mu_1)}$ *and* $a < \frac{c_2 - 1}{\nu_2(1-\mu_2)}$ *or* $a < \frac{c_1 - 1}{\nu_1(1-\mu_1)}$ *and* $a > \frac{c_2 - 1}{\nu_2(1-\mu_2)}$,
- *a non-hyperbolic node if* $a = \frac{c_1 - 1}{\nu_1(1-\mu_1)}$ *or* $a = \frac{c_2 - 1}{\nu_2(1-\mu_2)}$.

Proof. At the equilibrium point E_0 the Jacobian matrix (12) is given by

$$J(E_0) = \begin{bmatrix} 1 + \nu_1 a(1-\mu_1) - c_1 & 0 \\ 0 & 1 + \nu_2 a(1-\mu_2) - c_2 \end{bmatrix}.$$

As $J(E_0)$ is a diagonal matrix. Then the eigenvalues of $J(E_0)$ are $\lambda_1 = 1 + \nu_1 a(1-\mu_1) - c_1$ and $\lambda_2 = 1 + \nu_2 a(1-\mu_2) - c_2$. If $c_1 < 1 + \nu_1 a(1-\mu_1)$ and $c_2 < \nu_2 a(1-\mu_2)$, then E_0 is a repelling node. From the conditions shown on the eigenvalues, the rest of the results can be demonstrated based on the following theorem. □

Theorem 2. *When the Nash equilibrium point has positive coordinates, then the equilibrium points E_1 and E_2 are saddle points.*

Proof. Substituting E_1 in (12), we get

$$J(E_1) = \begin{bmatrix} 1 - \nu_1[a(1-\mu_1) - c_1] & -\frac{\nu_1(a(1-\mu_1) - c_1)}{2} \\ 0 & 1 + \frac{\nu_2}{2}[a(1-\mu_1)(1-\mu_2) + c_1(1-\mu_2) - 2c_2(1-\mu_1)] \end{bmatrix}.$$

The two eigenvalues of Jacobian matrix above are $\lambda_1 = 1 - \nu_1[a(1-\mu_1) - c_1]$ and $\lambda_2 = 1 + \frac{\nu_2}{2}[a(1-\mu_1)(1-\mu_2) + c_1(1-\mu_2) - 2c_2(1-\mu_1)]$. If the Nash equilibrium point has positive coordinates, hence $|\lambda_1| < 1$ and $|\lambda_2| > 1$. Therefore, the equilibrium point E_1 is a saddle point. In a certain manner, we can demonstrate that the E_2 is a saddle point too. This completes the proof. □

In order to study the local stability of the Nash equilibrium E_*, we calculate the Jacobian matrix at this point in the form:

$$\mathbf{J}(E_*) = \begin{bmatrix} 1 - 2\nu_1 b(1-\mu_1)q_1^* & -\nu_1 b(1-\mu_1)q_1^* \\ -\nu_2 b(1-\mu_2)q_2^* & 1 - 2\nu_2 b(1-\mu_2)q_2^* \end{bmatrix}.$$

Then the eigenvalues λ_1, λ_2 of this matrix are the roots of the following quadratic equation,

$$\lambda^2 - tr(\mathbf{J}(E_*))\lambda + Det(\mathbf{J}(E_*)) = 0,$$

where $tr(\mathbf{J}(E_*)) = 2 - 2\nu_1 b(1-\mu_1)q_1^* - 2\nu_2 b(1-\mu_2)q_2^*$ and $Det(\mathbf{J}(E_*)) = (1 - 2\nu_1 b(1-\mu_1)q_1^*)(1 - 2\nu_2 b(1-\mu_2)q_2^*) - \nu_1\nu_2 b^2(1-\mu_1)(1-\mu_2)q_1^*q_2^*$. We find $tr^2(\mathbf{J}(E_*)) - 4Det(\mathbf{J}(E_*)) = 4b^2[(\nu_1(1-\mu_1)q_1^* - \nu_2(1-\mu_2)q_2^*)^2 + \nu_1\nu_2(1-\mu_1)(1-\mu_2)q_1^*q_2^*]$. Since all parameters are definitely positive then the following discriminant is positive.

$$tr^2(\mathbf{J}(E_*)) - 4Det(\mathbf{J}(E_*)) > 0.$$

From above, it is easy to assume that the eigenvalues λ_1, λ_2 of this matrix $\mathbf{J}(E_*)$ are real eigenvalues. By the way of calculation, we get that:

$$1 - tr(\mathbf{J}(E_*)) + Det(\mathbf{J}(E_*)) = 3\nu_1\nu_2 b^2(1-\mu_1)(1-\mu_2)q_1^*q_2^* > 0,$$

When the Nash equilibrium point has positive coordinates, it's easy to see that the eigenvalues λ_1, λ_2 of $\mathbf{J}(E_*)$ are less than one. The local asymptotic stability of E_* is the following necessary condition:

$$1 + tr(\mathbf{J}(E_*)) + Det(\mathbf{J}(E_*)) = 4 - 4\nu_1 b(1-\mu_1)q_1^* - 4\nu_2 b(1-\mu_2)q_2^* + 3\nu_1\nu_2 b^2(1-\mu_1)(1-\mu_2)q_1^*q_2^* < 0. \quad (15)$$

The condition (15) defines the stability region for the Nash equilibrium point of the game (10). We can conclude the above result in the following theorem:

Theorem 3. *The Nash equilibrium point E_* of the game (8) is locally stable provided that:*

$$4 - 4\nu_1 b(1-\mu_1)q_1^* - 4\nu_2 b(1-\mu_2)q_2^* + 3\nu_1\nu_2 b^2(1-\mu_1)(1-\mu_2)q_1^*q_2^* < 0. \quad (16)$$

It is clear that if the condition $1 + tr(\mathbf{J}(E_*)) + Det(\mathbf{J}(E_*)) = 0$ satisfies the Nash equilibrium point E_*, it will undergo a flip bifurcation starting on period doubling cascade. Inequality (16) governs the stability of the dynamic game (8) when it is drawn for any pair of the system's parameters in the plane. The dynamical behaviors, phase portrait, bifurcation diagrams, critical curves and basin of attraction of model (8) will be shown in the next numerical simulation.

5. Numerical Simulation of Dynamic Game (8)

Since the system (8) has many parameters, we study in this section the influences of maximum price parameter a, the speed of adjustment parameter ν_1 and the sale constraint parameter μ_1 on the stability of Nash equilibrium point keeping the other parameters values fixed. This numerical experiments include using some popular graphs such as largest Lyapunov exponent (LLE), 1D bifurcation diagram, phase plane of chaotic attractors, and attraction basins for some periodic cycles. These graphs are important when studying the complex dynamic characteristics of such systems. We begin our analysis by investigating the influences of the sale's constraint parameter

μ_1 on the dynamics of the map (8). This requires to consider the following parameters set, $a = 11.25, b = 0.5, c_1 = 0.1, c_2 = 0.3, \mu_2 = 0.6, \nu_1 = 0.2$ and $\nu_2 = 0.7$. Since the fixed point E_* depends on the parameters a, b, c_1, c_2, μ_1 and μ_2 so it will be changed as we study the influence of μ_1 and its stability will be affected too. Taking μ_1 as the bifurcation parameter and at this parameters set, Figure 1a shows the 1D bifurcation diagram when varying this parameter. Experiment simulations show that the two parameters ν_1 and μ_1 have an opposite impact on the stability of the fixed point E_*. Taking the other parameters' values as previously and change μ_1 to 0.000215 the fixed point becomes $E_* = (7.866637992, 6.566681002)$ and the Jacobian gets,

$$\begin{bmatrix} -0.57299 & -0.78649 \\ -0.91934 & -0.83867 \end{bmatrix}$$

whose eigenvalues are $\lambda_+ \approx 0.15481$ and $\lambda_- \approx -1.56647$ with $|\lambda_+| < 1$ and $|\lambda_-| > 1$. This means that E_* is unstable saddle point. The dynamic behavior at this set of parameters' values including μ_1 is displayed in Figure 1b. It shows a two-piece chaotic attractor around the saddle fixed point. The light grey denotes the basin of E_* which includes holes of divergent and infeasible points. As μ_1 increases further the dynamic is converted into a four-piece chaotic attractor at $\mu_1 = 0.01075$. Figure 1c plots the basin of attraction of those four unconnected chaotic areas. As μ_1 increases those four chaotic areas change into a period-16 cycle. It has a quite complicated attraction basin at the same parameters set and $\mu_1 = 0.03$. Figure 1e,f display the attraction basin of period-4 and period-2 cycles. They are born at the same parameters' set and for $\mu_1 = 0.108$ and $\mu_1 = 0.89$ respectively. Keeping the other parameters' values fixed and change $\mu_1 = 0.828$ the fixed point becomes $E_* = (7.224806201, 6.887596899)$ and the Jacobian gets,

$$\begin{bmatrix} 0.75147 & -0.12427 \\ -0.96426 & -0.92853 \end{bmatrix}$$

whose eigenvalues are $\lambda_+ \approx 0.819996$ and $\lambda_- \approx -0.997057$ with $|\lambda_+| < 1$ and $|\lambda_-| < 1$. This means that E_* is local stable point. From this discussion we can see that there is an inverse period-doubling bifurcation that is merged when taking the sale's constraint μ_1 as the bifurcation parameter. Then the game (8) undergoes a chaos zone, quasi-period range, and comes back to a local stable state with an increasing in μ_1. Noting that the system (8) will return to stability from a chaotic state after many iterations of this system. Therefore the two competed firms should control the degree of minimum sales constraint parameter so as to avoid a market chaotic state. Furthermore the game (8) becomes more stable if the minimum sales constraint is considered by the players. On the other hand, the speed of adjustment ν_1 has given interesting results on the game's behavior. Numerical simulation examples show that when firms adjust the speed of a certain value, the Nash equilibrium point of the system (8) will lose its stability, the system will become unpredictable, and chaos may occur. It's difficult for firms to deal with such a complicated scenario. Consequently, the speed of adjustment to a very appropriate range must be taken into account by firms in order to avoid decreasing market efficiency and profits. We can conclude that the game (8) tends to exhibit more stability when at least one firm operates beyond its minimum sales constraint. Furthermore, the numerical simulation shows that the parameter a at the parameters' set, $b = 0.5, c_1 = 0.2, c_2 = 0.3, \mu_1 = \mu_2 = 0.6, \nu_1 = 0.5$ and $\nu_2 = 0.65$ makes the fixed point unstable due to flip bifurcation. Taking a as the bifurcation parameter, Figure 1g shows that the fixed point becomes stable for all a until a reaches the value on where period-2 cycle coexists. For further increase in a higher period cycles are born and routes to chaotic attractors are obtained. At $a = 12.11$ and the other set of parameters are fixed a two-piece chaotic attractor is coexisted as shown in Figure 1h. It is clear that its basin of attraction lies in a quadrilateral area that will be discussed later on in this section.

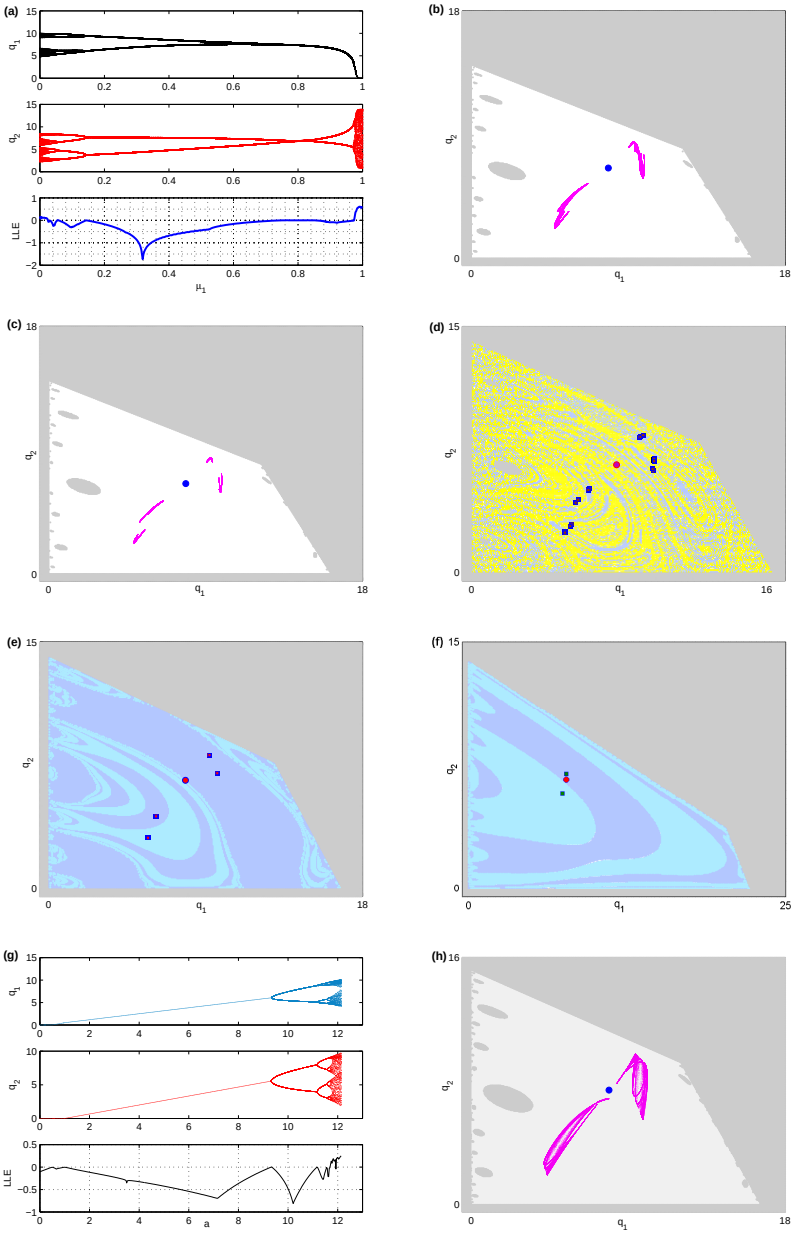

Figure 1. (**a**) Bifurcation diagram on varying the parameter μ_1. (**b**) The attraction basin of the two chaotic areas. (**c**) The attraction basin of the four chaotic areas. (**d**) The attraction basin of the period-16 cycle at $\mu_1 = 0.030$. (**e**) The attraction basin of period-4 cycle at $\mu_1 = 0.108$. (**f**) The attraction basin of period-2 cycle at $\mu_1 = 0.56$. Other parameters' values are $a = 11.25, b = 0.5, c_1 = 0.1, c_2 = 0.3, \mu_2 = 0.6, \nu_1 = 0.2$ and $\nu_2 = 0.7$. (**g**) Bifurcation diagram on varying the parameter a. (**h**) The attraction basin of the two chaotic areas at $a = 12.11$ while the other parameters' values are: $a = 11.25, b = 0.5, c_1 = 0.1, c_2 = 0.3, \mu_2 = 0.6, \nu_1 = 0.2$ and $\nu_2 = 0.7$.

We should highlight here that the system (8) can generate unbounded or negative trajectories if the initial condition $(q_{0,1}, q_{0,2})$ are assumed to be taken far from the origin. If $q_{i0} > \frac{1+\nu_i[(1-\mu_i)a-c_i]}{b\nu_i(1-\mu_i)}, i = 1, 2$ the first iteration of the system (8) gives negative values for $q_i(t+1)$. Therefore, successive iterations yield negative and decreasing values for the system (8) as $q_i(t+1) = q_i(t) + \nu_i q_i[(1-\mu_i)(a - 2bq_i - bq_j) - c_i] < q_i$ being $(1-\mu_i)a - c_i > 0$ if (11) holds. This means that attractors at finite distances are impossible to be globally attracting in $\mathbb{R}^2_+$ because their attraction basins can not be extended out the rectangle $[0, ((1-\mu_1)a - c_1)/b\nu_1(1-\mu_1)] \times [0, ((1-\mu_2)a - c_2)/b\nu_2(1-\mu_2)]$. The map (8) has

another important distinctive feature that is each axis $q_i(t) = 0$ gives $q_i(t+1) = 0, i = 1, 2$ that means $q_i(t)$ is mapped into itself and hence it is trapped. Setting $q_i(t) = 0$ (the monopoly case) in (8) we get

$$q_j(t+1) = \left[1 + \nu_j \left((1-\mu_j)a - c_j\right)\right] q_j(t) - 2b\nu_j(1-\mu_j)q_j^2(t) \ , j = 1, 2, \ \ i \neq j \tag{17}$$

The Equation (17) conjugates the standard logistic map, $y(t+1) = \lambda y(t)(1-y(t))$ through the linear transformation

$$q_j(t) = \frac{1 + \nu_j \left((1-\mu_j)a - c_j\right)}{2b\nu_j(1-\mu_j)} y(t) \tag{18}$$

where, $\lambda = 1 + \nu_j \left((1-\mu_j)a - c_j\right)$. This implies that the dynamic of (17) is governed by the well-known dynamics of standard logistic map. The map (17) is characterized as a unimodel map and $\frac{dq_j(t+1)}{dq_j(t)} = 0$ gives the unique critical point C_{-1} as follows

$$q_j^{C_{-1}} = \frac{1 + \nu_j \left((1-\mu_j)a - c_j\right)}{4b\nu_j(1-\mu_j)}, j = 1, 2 \tag{19}$$

which conjugates the critical point $y = \frac{1}{2}$ for the logistic map. There are two fixed points for the map (17) given by

$$\begin{array}{l} q_j^{E_o} = 0, \\ q_j^{E_j} = \frac{(1-\mu_j)a - c_j}{2b(1-\mu_j)} \end{array} \tag{20}$$

which conjugate the fixed points, $y = 0$ and $y = \frac{\nu_j\left((1-\mu_j)a - c_j\right)}{1+\nu_j\left((1-\mu_j)a - c_j\right)} = 1 - \frac{1}{\lambda}$ of the logistic map. It is easy to see that $\left|\frac{dq_j(t+1)}{dq_j(t)}\right|_{q_j = q_j^{E_o}} > 1$ and hence $q_j^{E_o}$ is unstable repelling point. The second fixed point of (20) is a stable attracting point provided that $0 < \nu_j \left((1-\mu_j)a - c_j\right) < 2$. At $\nu_j \left((1-\mu_j)a - c_j\right) > 2$ the dynamic behavior of (17) may be periodic cycle or cyclic chaotic behavior whose attraction basin is bounded by the unstable repelling point $q_j^{E_o}$ and its preimage O_{-1}^j whose coordinate is

$$q_j^{O_{-1}} = \frac{1 + \nu_j \left((1-\mu_j)a - c_j\right)}{2b\nu_j(1-\mu_j)} \tag{21}$$

which conjugates the point $y = 1$ in the standard logistic map. This implies that trajectories of the map (14) starting from an initial point selected out of the interval $[0, q_j^{O_{-1}}]$ are divergent to $-\infty$. Numerically, we assume the set of parameters' values, $a = 10, b = 0.3, c = 0.3$ and $\mu = 0.5$. Figure 1a shows that $q_j^{E_j}$ is locally asymptotically stable for all the value of ν till it approaches $\nu_j((1-\mu_j)a - c_j) = 2$ on where period-doubling bifurcation coexists. Taking ν as the bifurcation parameter of (17), Figure 2a shows that $q_j^{E_j}$ is locally stable for all the value of ν except at the point $\nu = \frac{2}{(1-\mu)a - c}$ where period-2 cycle is born due to flip bifurcation. As ν increases further chaotic attractors exist. Figure 2b shows a stable fixed point at the parameters' values, $a = 10, b = 0.3, c = 0.3, \mu = 0.5$ and $\nu = 0.4$. It is clear that the basin of the stable fixed point lies within the interval $[0, q_j^{O_{-1}}]$. Increasing ν to $\nu = 0.635$ gives rise to chaotic attractor with basin of attraction also lies within the same interval as shown in Figure 2c. On the other hand, when we take μ as the bifurcation parameter, Figure 2d shows the bifurcation diagram for the map (17) at the parameters' values, $a = 6, b = 0.5, c = 0.3$ and $\nu = 0.5$. At $\mu = 1 - \frac{\nu c - 2}{\nu a}$ a period-2 cycle is born. As μ increases further to $\mu = 0.25$ the fixed point gets stable as shown in Figure 2e. For $\mu = 0.018$ a chaotic attractor exists and its basin of attraction is also within the interval $[0, q_j^{O_{-1}}]$ as shown in Figure 2f.

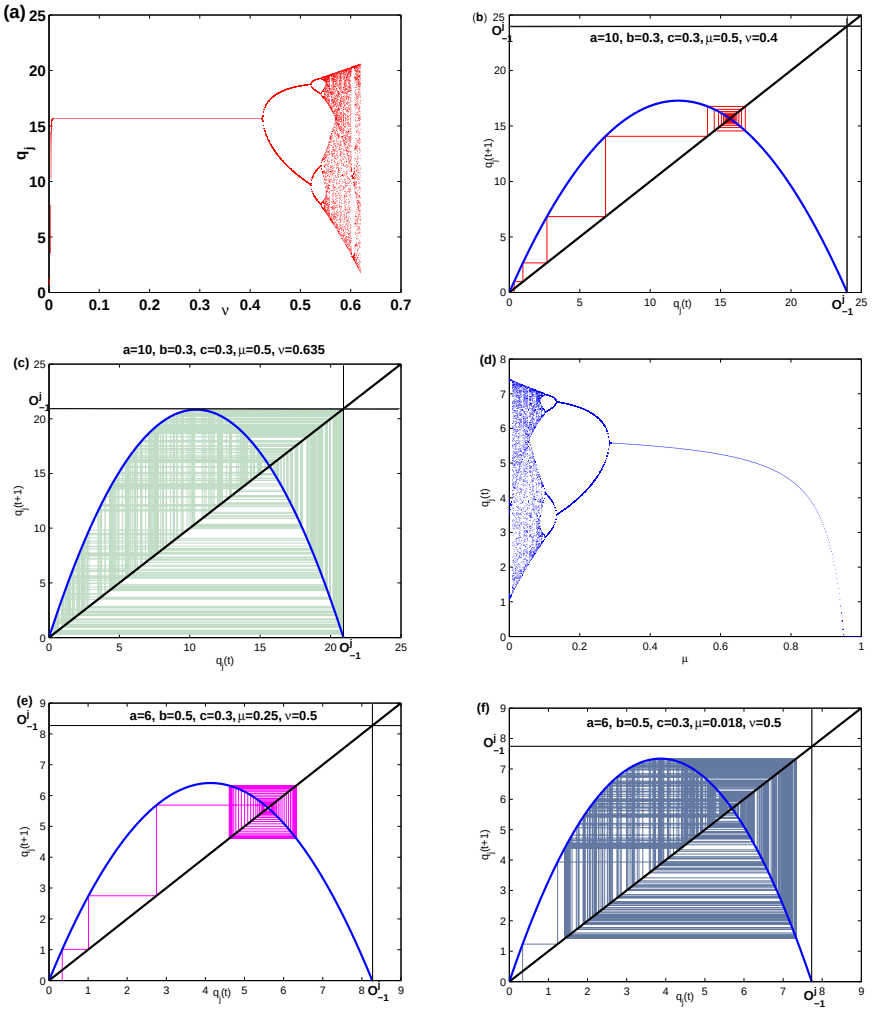

Figure 2. (**a**) The diagram of flip bifurcation taking ν as the bifurcation parameter. (**b**) The basin of attraction of the stable fixed point at $a = 10, b = 0.3, c = 0.3$, $\mu = 0.5$ and $\nu = 0.4$. (**c**) The basin of attraction of the unstable fixed point at $a = 10, b = 0.3, c = 0.3$, $\mu = 0.5$ and $\nu = 0.635$. (**d**) The diagram of bifurcation taking μ as the bifurcation parameter. (**e**) The basin of attraction of the stable fixed point at $a = 6, b = 0.5, c = 0.3$, $\nu = 0.5$ and $\mu = 0.25$. (**f**) The basin of attraction of the unstable fixed point at $a = 6, b = 0.5, c = 0.3$, $\nu = 0.5$ and $\mu = 0.018$.

Now we study the dynamics of (8) at different sets of parameters' values. Setting $a = 11, b = 0.5$, $c_1 = 0.2$, $c_2 = 0.3$, $\mu_1 = 0.6$, $\mu_2 = 0.6, \nu_1 = 0.33$ and $\nu_2 = 0.71$ we have only the stable E_* with its basin of attraction in Figure 3a. The light blue color consists of an open set of the points (q_1, q_2) in the phase plane whose trajectories $T(q_1, q_2)$ belong to the basin of attraction of E_* (which is denoted by $B(E_*)$). The grey color color denotes to the basin of infinity that contains all the points generating unbounded trajectories and is denoted by $B(\infty)$. This basin includes the divergent and unfeasible points. Figure 3b shows the basin of attraction of a chaotic attractor that coexists at the parameters' values, $a = 11, b = 0.5, c_1 = 0.2, c_2 = 0.3, \mu_1 = 0.6, \mu_2 = 0.6, \nu_1 = 0.715$ and $\nu_2 = 0.6$ while Figure 3c displays the basin of attraction of the period-8 cycle. As one can see from all those figures that their basins are bounded by line segments separate $B(\kappa)$ from $B(\infty)$ where κ refers to a bounded attracting set such as E_*, periodic cycles or any complex chaotic attractors around E_*. At the parameters set $a = 10.99, b = 0.5, c_1 = 0.47, c_2 = 0.3, \mu_1 = 0.6, \mu_2 = 0.6, \nu_1 = 0.72$ and $\nu_2 = 0.69$ we give in Figure 3d another quite complicated attractor around the fixed point, as one can see that it appears at $c_1 > c_2$. Now we assume another set of parameters' values that is $a = 11, b = 0.4, c_1 = c_2 = 0.33, \mu_1 = \mu_2 = 0.3$, and $\nu_1 = \nu_2 = 0.28$. This set indicates equality of the marginal costs, speed of adjustments and sales

constraints. Numerical simulations show that at this set a period-2 cycle is emerged with a basin of attraction that is bounded by the same previous segments. As the speed of adjustment parameters, the sales constraints have some influences on the dynamics of (8). For this reason we decrease μ_1 to 0.0086 to get four chaotic attractors that are represented in Figure 3e with the basin of attraction. Increasing μ_1 further to 0.001 we get two unconnected chaotic areas represented in Figure 2f with their basins. In conclusion, we have seen that $B(\infty)$ is an unconnected set which sometimes has unconnected regions represented by holes in Figure 3b,d,f.

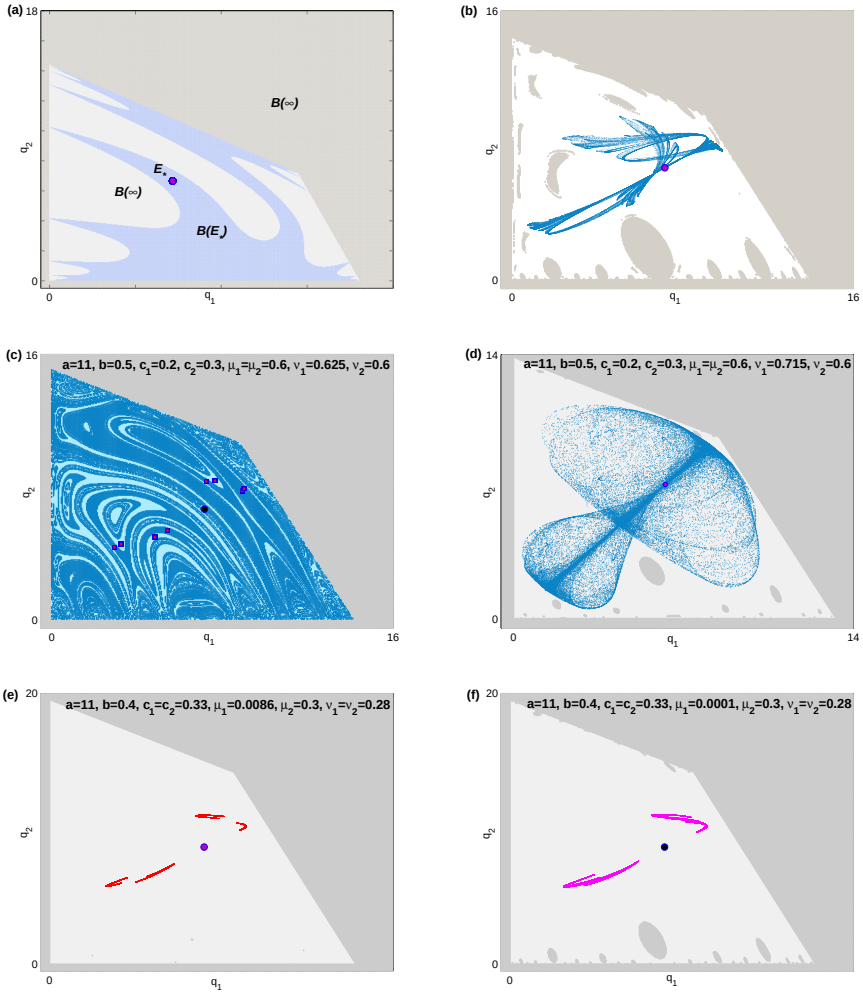

Figure 3. (**a**–**f**) Numerical representations of κ at different sets of parameters' values .

Now we intend to identify the structure of attraction basin for the map (8) and show the regions on where the map's phase plane can be divided. Since the map (8) is trapped in the point $(0,0)$ so it is important to calculate the rank-1 preimages for this point. The preimages of point (0,0) can be derived by algebraically solving the following system,

$$\begin{aligned} q_1 + \nu_1 q_1[(1-\mu_1)(a-2bq_1-bq_2)-c_1] &= 0, \\ q_2 + \nu_2 q_2[(1-\mu_2)(a-2bq_2-bq_1)-c_2] &= 0, \end{aligned} \tag{22}$$

which gives four preimages, $O_{-1}^{(0)} = (0,0), O_{-1}^{(1)} = (q_1^{O_{-1}}, 0), O_{-1}^{(2)} = (0, q_2^{O_{-1}})$, and $O_{-1}^{(3)} = (\hat{q}_1, \hat{q}_2)$ where,

$$\begin{aligned} \hat{q}_1 &= \frac{a(1-\mu_1)(1-\mu_2)+c_2(1-\mu_1)-2c_1(1-\mu_2)}{3b(1-\mu_1)(1-\mu_2)} + \frac{2\nu_2(1-\mu_2)-\nu_1(1-\mu_1)}{3b\nu_1\nu_2(1-\mu_1)(1-\mu_2)}, \\ \hat{q}_2 &= \frac{a(1-\mu_1)(1-\mu_2)+c_1(1-\mu_2)-2c_2(1-\mu_1)}{3b(1-\mu_1)(1-\mu_2)} + \frac{2\nu_1(1-\mu_1)-\nu_2(1-\mu_2)}{3b\nu_1\nu_2(1-\mu_1)(1-\mu_2)}. \end{aligned} \tag{23}$$

Or,

$$\begin{array}{l}\hat{q}_1 = q_1^* + \frac{2\nu_2(1-\mu_2)-\nu_1(1-\mu_1)}{3b\nu_1\nu_2(1-\mu_1)(1-\mu_2)},\\ \hat{q}_2 = q_2^* + \frac{2\nu_1(1-\mu_1)-\nu_2(1-\mu_2)}{3b\nu_1\nu_2(1-\mu_1)(1-\mu_2)}.\end{array} \tag{24}$$

Now, the preimages of any point $(p, 0)$ on the invariant axis $q_2 = 0$ can be obtained by algebraic solution of the system,

$$\begin{array}{l}q_1 + \nu_1 q_1[(1-\mu_1)(a - 2bq_1 - bq_2) - c_1] = p,\\ q_2 + \nu_2 q_2[(1-\mu_2)(a - 2bq_2 - bq_1) - c_2] = 0.\end{array} \tag{25}$$

The second Equation of (25) gives $q_2 = 0$ or,

$$1 + \nu_2[(1-\mu_2)a - c_2] - b\nu_2(1-\mu_2)q_1 - 2b\nu_2(1-\mu_2)q_2 = 0. \tag{26}$$

With $q_2 = 0$ we get the following quadratic equation,

$$-2b\nu_1(1-\mu_1)q_1^2 + (1 + \nu_1\left[a(1-\mu_1) - c_1\right])q_1 - p = 0, \tag{27}$$

which has the following discriminant,

$$\Delta = \left[1 + \nu_1\left(a(1-\mu_1) - c_1\right)\right]^2 - 8bp v_1(1-\mu_1). \tag{28}$$

This means the point $(p, 0)$ has on the same axis no rank-1 preimages, two distinct rank-1 preimages or two coincided rank-1 preimages if $\Delta < 0, \Delta > 0$ or $\Delta = 0$ respectively. It may have also four preimages two of which lie on the same axis and the other two on the line (26). The same discussion and observation are for any point in the form $(0, p)$. The above discussion gives the following proposition.

Proposition 1. *Let the line segments ξ_1 and ξ_2 be $\xi_1 = O_{-1}^{(0)}O_{-1}^{(1)}$ and $\xi_2 = O_{-1}^{(0)}O_{-1}^{(2)}$ then*

$$\Im = \left(\bigcup_{n=0}^{\infty} T^{-n}(\xi_1)\right) \cup \left(\bigcup_{n=0}^{\infty} T^{-n}(\xi_2)\right),$$

be the set of all preimages of rank-n.

Figure 4 shows that the line segments ξ_1, ξ_2 and their rank-1 preimages ξ_1^{-1}, ξ_2^{-1} constitute a quadrilateral region $O_{-1}^{(0)}O_{-1}^{(1)}O_{-1}^{(3)}O_{-1}^{(2)}$ that is exactly the attraction basin of the chaotic attractor given in the figure. Those segments and their rank-1 preimages construct the whole boundary of $\Im$.

Now we put the map (8) in the following form,

$$\begin{array}{l}\acute{q}_1 = q_1 + \nu_1 q_1[(1-\mu_1)(a - 2bq_1 - bq_2) - c_1],\\ \acute{q}_2 = q_2 + \nu_2 q_2[(1-\mu_2)(a - 2bq_2 - bq_1) - c_2]\end{array} \tag{29}$$

where $'$ refers to the time evolution. Solving algebraically (29) with respect to q_1 and q_2 one can get $0, 2$ and 4 real preimages. It means that the map (29) is noninvertible and the phase plane may be divided into three zones Z_0, Z_2 and Z_4. In order to identify these zones we should calculate the critical curves LC and LC_{-1}. LC_{-1} is obtained by solving $det(J) = 0$ that gives the following hyperbola,

$$\begin{array}{l}q_1^2 + q_2^2 + q_1q_2 + \Delta_1 q_2 + \Delta_2 q_1 + \Delta_3 = 0,\\ \Delta_1 = \frac{\nu_1\nu_2[5(1-\mu_1)(1-\mu_2)a - c_2(1-\mu_1) - 4c_1(1-\mu_2)] + \nu_1(1-\mu_1) + 4\nu_2(1-\mu_2)}{-4b\nu_1\nu_2(1-\mu_1)(1-\mu_2)},\\ \Delta_2 = \frac{\nu_1\nu_2[5(1-\mu_1)(1-\mu_2)a - 4c_2(1-\mu_1) - c_1(1-\mu_2)] + 4\nu_1(1-\mu_1) + \nu_2(1-\mu_2)}{-4b\nu_1\nu_2(1-\mu_1)(1-\mu_2)},\\ \Delta_3 = \frac{a\nu_1\nu_2[(1-\mu_1)(1-\mu_2)a - c_2(1-\mu_1) - c_1(1-\mu_2)] + 1 - c_1\nu_1 - c_2\nu_2 + c_1c_2\nu_1\nu_2}{-4b\nu_1\nu_2(1-\mu_1)(1-\mu_2)}\end{array} \tag{30}$$

Now LC is obtained from $LC = T(LC_{-1})$. The complicated form of the hyperbola makes us to plot LC_{-1} at the parameters' set, $a = 11, b = 0.5, c_1 = 0.2, c_2 = 0.3, \mu_1 = \mu_2 = 0.6, \nu_1 = 0.33$ and $\nu_2 = 0.71$. Figure 5. displays the zones Z_0, Z_2, Z_4 and the critical curves. The fixed point at this set of parameters' values belongs to Z_2.

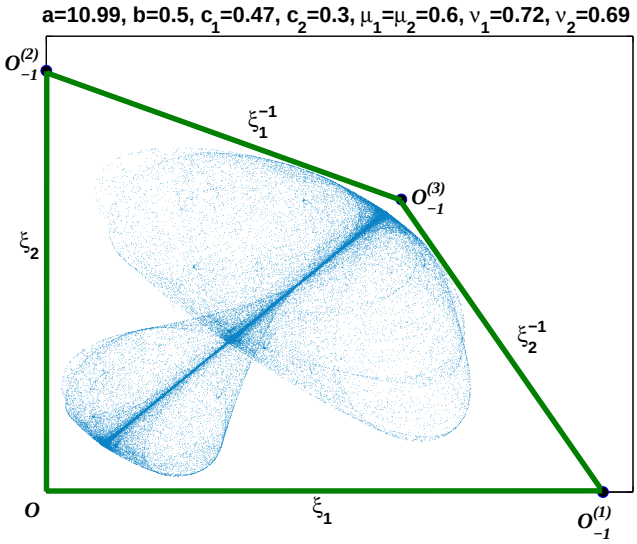

Figure 4. The whole boundary of the basin of attraction of the chaotic attractor at the parameters' values, $a = 10.99, b = 0.5$, $c_1 = 0.47$, $c_2 = 0.3$, $\mu_1 = 0.6$, $\mu_2 = 0.6, \nu_1 = 0.72$ and $\nu_2 = 0.69$.

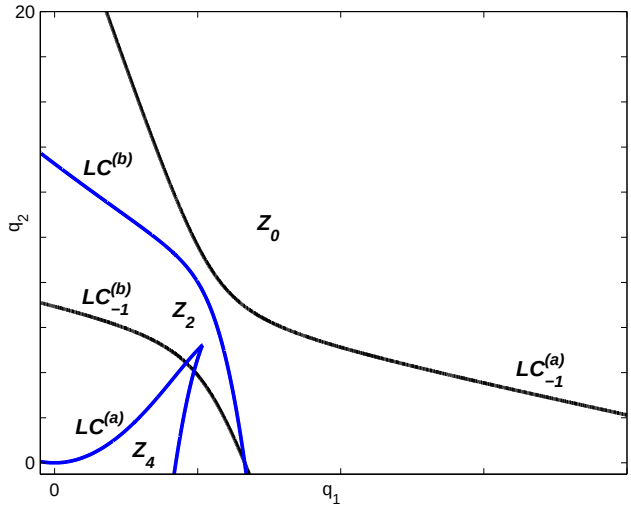

Figure 5. The zones of the preimages and critical curves LC and LC_{-1} at the parameters' values, $a = 11, b = 0.5, c_1 = 0.2, c_2 = 0.3, \mu_1 = \mu_2 = 0.6, \nu_1 = 0.33$ and $\nu_2 = 0.71$.

6. Conclusions

In this paper, we have developed the Bischi–Naimzada duopoly game where competitors can maximize local profits under minimal sales constraints. We have studied and calculated the stability conditions of equilibrium points of this game. On the basis of nonlinear dynamical systems theory, we have examined the effects of critical system parameters on the stability and complexity of the dynamic game model, both in terms of sales constraints and speeds of adjustment. Using numerical analysis, the qualitative behaviors of the model dynamics have been explored by bifurcation diagrams, phase diagrams and largest Lyapunov exponent. In addition, the phase level of the map which

was divided into three zones Z_0, Z_2 and Z_4 as a result of the noninvertible game has been analyzed. Research and analytical simulations show that the sensitive dependence of the dynamics of the model on both the speeds of adjustment and the parameters of the sales constraints. It also showed that, in contrast to the sales constraint parameters with an increase which has a stabilizing effect, the adjustment speeds have an effect of instability on the dynamics of model. In our contribution, it has been found that the Bischi–Naimzada competition game model that takes into account sales constraints and maximizes the profit function is much more stable around the Nash equilibrium than the same model that does not take into account sales constraints. In oligopolistic games, limited rational expectations are important for the investigation of market dynamics subject to minimal sales constraints. These games are of great importance for the study of competition between airlines, banking, music, drinks and telecommunications companies. This is for simple reason that is firms in previous areas always want to maximize profits with a minimum of sales. The extension of this paper is to explore of heterogeneous behaviors in such competitive Cournot games on the basis of minimal sales. More realistic conditions need to be taken into account, such as team participation, random selection of expectations, reduced risk, increase revenue and chaos control. Such important issues will be investigated in this direction for future studies.

Author Contributions: Both authors have contributed equally to this work. All authors have read and agreed to the published version of the manuscript.

Funding: Deanship of Scientific Research at king Saud University, Research group NO (RG-1438-046).

Acknowledgments: The authors would like to extend their sincere appreciation to the Deanship of Scientific Research at king Saud University for its funding this Research group NO (RG-1438-046).

Conflicts of Interest: The authors declare no conflict of interest.

References

1. Cournot, A.A. Researches into the principles of the theory of wealth. In *Classics in Economics*; Augustus M Kelley Pubs.: New York, NY, USA, 1971.
2. Rand, D. Exotic phenomena in games and duopoly models. *Math. Econ.* **1978**, *5*, 173–184. [CrossRef]
3. Puu, T. Chaos in duopoly pricing. *Chaos Solitons Fractals* **1991**, *1*, 573–581. [CrossRef]
4. Lorenz, H.W. *Nonlinear Dynamical Economics and Chaotic Motion*; Springer: Berlin, Germany, 1993.
5. Kopel, M. Simple and complex adjustment dynamics in Cournot duopoly models. *Chaos Solitons Fractals* **1996**, *7*, 2031–2048. [CrossRef]
6. Ahmed, E.; Agiza, H.N. Dynamics of a Cournot game with n-competitors. *Chaos Solitons Fractals* **1998**, *9*, 1513–1517. [CrossRef]
7. Puu, T. The chaotic duopolists revisited. *J. Econ. Organ.* **1998**, *33*, 385–394. [CrossRef]
8. Agiza, H.N. Explicit stability zones for Cournot game with 3 and 4 competitors. *Chaos Solitons Fractals* **1998**, *9*, 1955–1966. [CrossRef]
9. Bischi, G.I.; Mammana, C.; Gardini, L. Multistability and cyclic attractors in duopoly games. *Chaos Solitons Fractals* **2000**, *11*, 543–564. [CrossRef]
10. Agliari, A.; Gardini, L.; Puu, T. The dynamics of a triopoly Cournot game. *Chaos Solitons Fractals* **2000**, *11*, 2531–2560. [CrossRef]
11. Bischi, G.I.; Naimzada, A. Global analysis of a dynamic duopoly game with bounded rationality. In *Advances in Dynamic Games and Applications*; Birkhauser: Boston, MA, USA, 2000; Volume 5.
12. Agiza, H.N.; Hegazi, A.S.; Elsadany, A.A. Complex dynamics and synchronization of a duopoly game with bounded rationality. *Math. Comput. Simul.* **2002**, *58*, 133–146. [CrossRef]
13. Agiza, A.N.; Elsadany, A.A. Nonlinear dynamics in the Cournot duopoly game with heterogenous players. *Physica A* **2003**, *320*, 512–524. [CrossRef]
14. Bischi, G.I.; Gallegati, M.; Naimzada, A. Symmetry-breaking bifurcations and representativefirm in dynamic duopoly games. *Ann. Oper. Res.* **1999**, *89*, 252–271. [CrossRef]
15. Bischi, G.I.; Gardini, L.; Kopel, M. Analysis of global bifurcations in a market share attraction model. *J. Econ. Dyn. Control* **2000**, *24*, 855–879. [CrossRef]

16. Puu, T. The chaotic monopolist. *Chaos Solitons Fractals* **1995**, *5*, 35–44. [CrossRef]
17. Ahmed, E.; Elettreby, M.F. Controls of the complex dynamics of a multi-market Cournot model. *Econ. Model.* **2014**, *37*, 251–254. [CrossRef]
18. Fanti, L.; Gori, L.; Sodini, M. Nonlinear dynamics in a Cournot duopoly with isoelastic demand. *Math. Comput. Simul.* **2015**, *108*, 129–143. [CrossRef]
19. Askar, S.S.; Al-Khedhairi, A. Analysis of nonlinear duopoly games with product differentiation: Stability, global dynamics, and control. *Discret. Dyn. Nat. Soc.* **2017**, *2017*, 2585708. [CrossRef]
20. Ma, J.; Zhang, F.; He, Y. Complexity analysis of a master-slave oligopoly model and chaos control. *Abstr. Appl. Anal.* **2014**, *2014*, 970205. [CrossRef]
21. Agliari, A.; Gardini, L.; Puu, T. Global bifurcations of basins in a triopoly game. *Int. J. Bifurcat. Chaos* **2002**, *12*, 2175–2207. [CrossRef]
22. Askar, S.S. The impact of cost uncertainty on Cournot duopoly game with concave demand function. *J. Appl. Math.* **2013**, *2013*, 809795. [CrossRef]
23. Andaluz, J.; Elsadany, A.A.; Jarne, G. Nonlinear Cournot and Bertrand-type dynamic triopoly with differentiated products and heterogeneous expectations. *Math. Comput. Simul.* **2017**, *132*, 86–99. [CrossRef]
24. Baiardi, L.C.; Naimzada, A.K. An oligopoly model with rational and imitation rules. *Math. Comput. Simul.* **2019,** *156*, 254–278. [CrossRef]
25. Zhou, J.; Zhou, W.; Chu, T.; Chang, Y.X.; Huang, M.J. Bifurcation, intermittent chaos and multi-stability in a two-stage Cournot game with R&D spillover and product differentiation. *Appl. Math. Comput.* **2019**, *341*, 358–378.
26. Al-Khedhairi, A. Dynamics of a Cournot duopoly game with a generalized bounded rationality. *Complexity* **2020**, *2020*, 8903183. [CrossRef]
27. Askar, S.S. The influences of asymmetric market information on the dynamics of duopoly game. *Mathematics* **2020**, *8*, 1132. [CrossRef]
28. Naimzada, A.; Sbragia, L. Oligopoly games with nonlinear demand and cost functions: Two boundedly rational adjustment processes. *Chaos Solitons Fractals* **2006**, *29*, 707–722. [CrossRef]
29. Tramontana, F. Heterogeneous duopoly with isoelastic demand function. *Econ. Model.* **2010**, *27*, 350–357. [CrossRef]
30. Askar, S.S. On Cournot-Bertrand competition with differentiated products. *Ann. Oper. Res.* **2014**, *223*, 81–93. [CrossRef]
31. Askar, S.S.; Alshamrani, A.M. The dynamic of economic games based on product differentiation. *J. Comput. Appl. Math.* **2014**, *268*, 135–144. [CrossRef]
32. Ahmed, E.; Elsadany, A.A.; Puu, T. On Betrand duopoly game with differentiated goods. *Appl. Math. Comput.* **2015**, *251*, 169–179.
33. Ma, J.; Si, F. Complex Dynamics of a Continuous Bertrand Duopoly Game Model with Two-Stage Delay. *Entropy* **2016**, *18*, 266. [CrossRef]
34. Peng, Y.; Lu, Q.; Xiao, Y.; Wu, X. Complex dynamics analysis for a remanufacturing duopoly model with nonlinear cost. *Phys. A Stat. Mech. Appl.* **2019**, *514*, 658–670. [CrossRef]
35. Ueda, M. Effect of information asymmetry in Cournot duopoly game with bounded rationality. *Appl. Math. Comput.* **2019**, *362*, 124535. [CrossRef]
36. Baumol, W.J. *Business Behavior, Value and Growth*; MacMillan Co.: New York, NY, USA, 1959.
37. Fisher, F.M. Review of Baumol's rst edition of Business Behavior, Value and Growth. *J. Political Econ.* **1960**, *68*, 314–315. [CrossRef]
38. Fisher, F.M. Comment on the goals of the rm. *Q. J. Econ.* **1965**, *79*, 500–503. [CrossRef]
39. Ahmed, E.; Hegazi, A.S.; El-Hafez, A.T.A. On multiobjective oligopoly. *Nonlinear Dyn. Psychol. Life Sci.* **2003**, *7*, 205–219. [CrossRef]
40. Ahmed, E.; Hegazi, A.S.; Abd El-Hafez, A.T. On Persistence In Multiobjective Oligopoly. *Int. J. Mod. Phys. C* **2001**, *12*, 901–907. [CrossRef]
41. Ahmed, E.; Ashry, G.A.; Askar, S.S. On multi-objective optimization and game theory in production management. *Int. J. Nonlinear Sci.* **2017**, *24*, 29–33.
42. Mert, M. What does a firm maximize? A simple explanation with regard to economic growth. *Int. J. Eng. Bus. Manag.* **2018**, *10*, 1–13. [CrossRef]

43. Ibrahim, A. Local stability condition of the equilibrium of a constraint profit maximization duopoly model. *AIP Conf. Proc.* **2019**, *2138*, 030020.
44. Tian, Y.; Ma, J.; Xie, L.; Koivumaki, T.; Seppanen, V. Coordination and control of multi-channel supply chain driven by consumers' channel preference and sales effort. *Chaos Solitons Fractals* **2020**, *132*, 109576. [CrossRef]
45. Pansera, B.A.; Guerrini, L.; Ferrara, M.; Ciano, T. Bifurcation Analysis of a Duopoly Game with R & D Spillover, Price Competition and Time Delays. *Symmetry* **2020**, *12*, 257.
46. Szidarovszky, F.; Bischi, G.I. *Games and Dynamics in Economics*; Springer: Berlin/Heidelberg, Germany, 2020.
47. Kalinowski, S. Price Discount for the Increased Order as a Cooperative Game in Bilateral Monopoly. *Econ. Sociol.* **2015**, *8*, 108–118. [CrossRef]
48. Ners, D. Coalitional Games, Excessive Competition and a Lack of Trust: An Experimental Approach. *Econ. Sociol.* **2017**, *10*, 227–238. [CrossRef] [PubMed]
49. Bischi, G.I.; Chiarella, C.; Kopel, M.; Szidarovszky, F. *Nonlinear Oligopolies: Stability and Bifurcations*; Springer Science & Business Media: Berlin/Heidelberg, Germany, 2009.
50. Hommes, C. *Behavioral Rationality and Heterogeneous Expectations in Complex Economic Systems*; Cambridge University Press: Cambridge, UK, 2013.